

Paper submitted to Wind Energy

# Modelling of offshore wind turbine wakes with the wind farm program FLaP

by

Bernhard Lange  
University of Oldenburg, Oldenburg, Germany

Hans-Peter Waldl  
University of Oldenburg, Oldenburg, Germany  
now at: Overspeed GmbH, Oldenburg, Germany

Rebecca Barthelmie  
Risø National Laboratory, Roskilde, Denmark

Algert Gil Guerrero  
University of Oldenburg, Oldenburg, Germany

Detlev Heinemann  
University of Oldenburg, Oldenburg, Germany

Corresponding author address:

Bernhard Lange  
University of Oldenburg  
Faculty of Physics  
Department of Energy and Semiconductor Research  
D-26111 Oldenburg  
Germany  
Phone: +49-441-798 3927  
Fax: +49-441-798 3326  
e-mail: Bernhard.Lange@uni-oldenburg.de

## Abstract

The wind farm layout program FLaP (Farm Layout Program) estimates the wind speed at any point in a wind farm and the power output of the turbines. The ambient flow conditions and the properties of the turbines and the farm are used as input. The core of the program is an axis-symmetric wake model, describing the wake behind one rotor. Here an approach based on the simplified Reynolds equation with an eddy-viscosity closure is chosen. The single wake model is combined with a model for the vertical wind speed profile and a wind farm model, which takes care of the interaction of all wakes in a wind farm.

The wake model has been extended to improve the description of wake development in offshore conditions, especially the low ambient turbulence and the effect of atmospheric stability. Model results are compared with measurements from the Danish offshore wind farm Vindeby. Vertical wake profiles and mean turbulence intensities in the wake are compared for single, double and quintuple wake cases with different mean wind speed, turbulence intensity and atmospheric stability.

It is found that within the measurement uncertainties the results of the wake model compare well with the measurements for the most important ambient conditions. The effect of the low turbulence intensity offshore on the wake development is modelled well for the Vindeby wind farm. Deviations are found when atmospheric stability deviates from near-neutral conditions. For stable atmospheric conditions both the free vertical wind speed profile and the wake profile are not modelled satisfactorily.

Key Words: Offshore, wind farm, wake model, Vindeby, turbulence intensity, atmospheric stability

## Notation

$u$	$[\text{ms}^{-1}]$	axial component of the flow velocity
$v$	$[\text{ms}^{-1}]$	radial component of the flow velocity
$x$	$[\text{m}]$	axial distance to the rotor plane
$r$	$[\text{m}]$	radial distance to the wake centreline.
$\overline{u'v'}$	$[\text{m}^2\text{s}^{-2}]$	Reynolds stress cross correlation
$\kappa$	-	von Karman constant (taken as 0.4)
$u_*$	$[\text{ms}^{-1}]$	friction velocity
$z$	$[\text{m}]$	height
$\Phi_m$	-	non-dimensional wind shear according to Monin-Obukhov theory
$L$	$[\text{m}]$	Monin-Obukhov length
$k$	-	empirical constant
$r_w$	$[\text{m}]$	wake radius
$u_0$	$[\text{ms}^{-1}]$	free flow wind speed at hub height
$u_c$	$[\text{ms}^{-1}]$	centreline velocity in the wake
$u_w$	$[\text{ms}^{-1}]$	axial velocity in the wake

$F(x)$	-	empirical filter function for wake eddy viscosity
$\varepsilon$	$[\text{m}^2\text{s}^{-1}]$	eddy-viscosity
$\varepsilon_a$	$[\text{m}^2\text{s}^{-1}]$	ambient eddy-viscosity
$\varepsilon_w$	$[\text{m}^2\text{s}^{-1}]$	wake eddy-viscosity generated by the wind shear in the wake
$k_M$	$[\text{m}^2\text{s}^{-1}]$	eddy diffusivity of momentum in the atmosphere
$c_t$	-	thrust coefficient of the rotor
$I$	-	turbulence intensity in the flow $\sigma_u/u$
$A$	$[\text{m}^2]$	rotor area
$u_{\text{Rotor}}$	$[\text{ms}^{-1}]$	wind speed averaged over the rotor area of a turbine with incident wake(s)
$\sigma_u$	$[\text{ms}^{-1}]$	standard deviation of $u$
$x_n$	$[\text{m}]$	near wake length
$x_H$	$[\text{m}]$	length of the first region of the near wake
$r_0$	$[\text{m}]$	radius of fully expanded rotor disk
$D$	$[\text{m}]$	rotor diameter
$B$	-	number of blades
$\lambda$	-	tip speed ratio
$z_H$	$[\text{m}]$	hub height
$I_a$	-	ambient turbulence intensity

$I_{\text{add}}$	-	added turbulence intensity in the wake
$I_{\text{a,n}}$	-	ambient turbulence intensity in neutral conditions
$I_{\text{add,n}}$	-	added turbulence intensity in the wake in neutral conditions
$I_{\text{a,input}}$	-	ambient turbulence intensity used as input to the wake model
$\Psi(z/L)$	-	stability function according to Monin-Obukhov theory
$z_0$	[m]	surface roughness length
$z_{\text{ref}}$	[m]	reference height

## 1 Introduction

For planning of large offshore wind farms, modelling of wake losses is an important part of the production estimation. Additionally, an estimation of turbulence intensity in the wind farm is essential for the load assumptions used in the design of the turbines. Some knowledge and considerable experience has been gained in the estimation of these wake effects from wind farms on land, which is available in wind farm models like PARK [1], Windfarmer [2] and FLaP [3].

Some differences exist between the atmospheric flow on land and offshore. To incorporate these effects the wind farm modelling program FLaP has been extended. Two characteristics of the offshore conditions are of paramount importance for the wake development: Sea surface roughness and atmospheric stability.

The roughness of water surfaces is different from land surfaces in that it is much smaller and dependent on the wave field, which in turn depends mainly on wind speed, but also on fetch, water depth, etc. (see e.g. [4]). This has been taken into account in the description of the ambient vertical wind speed profile. It also has important consequences for the modelling of the wake since it leads to a low and wind speed dependent turbulence intensity. In offshore conditions atmospheric stratification departs from near-neutral also for higher wind speeds, which are important for wind power production. This has been included in the modelling of the ambient flow and also might have an influence on the wake development.

For the modelling of the ambient atmospheric flow standard Monin-Obukhov similarity theory (see e.g. [5]) has been used in FLaP, employing the Charnock relation [6] to

estimate the sea surface roughness. A two-dimensional, axis-symmetric wake model with eddy-viscosity closure is used, based on the model described by Ainslie [7]. It has been extended to improve the modelling of the influence of turbulence intensity and atmospheric stability on the wake. Comparisons of model results with results of several other wake models and comparisons of results before and after the improvements are made ([8], [9]) in the framework of the ENDOW project [10].

Model results have been compared with measurements at the offshore wind farm Vindeby for a wide range of ambient conditions. Measurements were available for single, double and quintuple wakes for different ambient wind speeds, turbulence intensities and atmospheric stability conditions. Vertical wind speed profiles in the wake and mean turbulence intensities are compared. The different parts of the wake model, namely the free flow model, the single wake model, the multiple wake model and the turbulence intensity model, have been considered separately where possible.

The plan of the paper is as follows: In the next chapter the wind farm model FLaP and the extensions made for offshore application are described. Section 3 contains a brief description of the measurements of Vindeby wind farm used for comparisons with the wake model. The results of the comparisons are summarised in section 4. Conclusions are drawn in the final chapter.

## 2 The FLaP wind farm model

### 2.1 Overview

For modelling the wind speed and turbulence intensity in a wake the wind farm modelling program FLaP (Farm Layout Program) [3] has been used. For a detailed

description of the program and validation see [11]. The program estimates wind speeds and turbulence intensities in wakes and their effect on the power output of the turbines in a wind farm. Core of any wind farm model is the description of the wake behind a rotor. An approach based on Ainslie [7] is used here. The concept of the model is to solve the governing equations of the flow numerically with suitable simplifications to allow fast computation.

Three sub-models are used to model the wind speed at any point in the farm and the respective power output of a turbine:

- Free flow model: For wind speeds at heights different from the hub height the vertical wind speed profile of the free flow is taken into account by convoluting the calculated wind speed in the wake with the incident ambient wind speed profile.
- Single wake model: It is used to calculate an axis-symmetric wake profile for any position behind the rotor.
- Multiple wake model: For multiple wakes the wind speed incident on a rotor, which is influenced by wakes of upwind turbines, is calculated from modelled wake deficits of the incident wakes. This wind speed is then taken as the new ‘ambient’ wind speed for this rotor, which is also used to calculate the power output of the turbine.

## 2.2 The free vertical wind speed profile

In the surface layer the vertical wind speed profile can be described with Monin-Obukhov theory by a logarithmic profile modified for the influence of atmospheric stability:

$$u(z) = \frac{u_*}{\kappa} \left[ \ln\left(\frac{z}{z_0}\right) - \Psi\left(\frac{z}{L}\right) \right] \quad (1)$$

The stability function  $\Psi(z/L)$  is calculated by the standard approach (see e.g. [5]).

The surface roughness of the sea is - in contrary to land surfaces - dependent on the sea state, which in turn depends on the wind speed and other influences. The classical approach for the estimation of the sea surface roughness by Charnock [6] is used:

$$z_0 = z_{ch} \frac{u_*^2}{g} \quad (2)$$

For the Charnock constant  $z_{ch}$  the standard value of 0.018 is taken [12]. Thus a vertical wind speed profile is found which includes stability influences and the wind speed dependent surface roughness.

### 2.3 Axis-symmetric single wake model

#### Improvements for offshore conditions

The Ainslie wake model has been extended for the use in offshore conditions in three ways:

- Ainslie [7] proposed a fixed near wake length of 2 rotor diameters (D). For offshore conditions the ambient turbulence intensity can be much lower than on land. This leads to a slower wake recovery and therefore to a longer near wake. The model has therefore been extended by an estimation of the near wake length using an approach proposed by Vermeulen [13].
- Because of the lower ambient turbulence, the modelling of the turbulence in the wake becomes more important. The Ainslie model has been extended to estimate the

wake turbulence intensity, calculated directly from the eddy-viscosity of the Ainslie model.

- For offshore conditions, atmospheric stability plays a more important role than on land, since non-neutral stratification occurs more frequently at higher wind speeds, which are important for wind energy utilisation. The influence of atmospheric stability on wake development has therefore been included in the model by assuming that ambient and wake generated eddy-viscosity are affected by atmospheric stability in the same way.

#### Differential equations describing the wake flow

The wake is considered to be axis-symmetric, which allows a two-dimensional formulation of the problem in cylindrical co-ordinates. To allow fast computation, a number of further assumptions are made. The flow is considered incompressible, without external forces or pressure gradients. Gradients of the standard deviation  $\overline{u'^2}$  and viscous terms are neglected. The flow can then be described with the two-dimensional Reynolds equation in the thin shear layer approximation without viscous terms in cylindrical co-ordinates:

$$u \frac{\partial u}{\partial x} + v \frac{\partial u}{\partial r} = -\frac{1}{r} \frac{\partial (r \overline{u'v'})}{\partial r} \quad (3)$$

This equation is combined with the continuity equation for incompressible fluids to form the differential equation system, which is solved numerically to model the wake flow.

$$\frac{\partial u}{\partial x} + \frac{1}{r} \frac{\partial (rv)}{\partial r} = 0 \quad (4)$$

Turbulence closure: Eddy-viscosity

The Reynolds-stress  $\overline{u'v'}$ , which indicates momentum transport across the flow, is modelled with the eddy-viscosity approach:

$$-\overline{u'v'} = \varepsilon \frac{\partial u}{\partial r} \quad (5)$$

Ainslie [7] splits the total eddy-viscosity  $\varepsilon$  into two components: the ambient eddy-viscosity of the atmospheric flow and the eddy-viscosity generated by the wind shear in the wake. The ambient eddy-viscosity is identified with the eddy diffusivity of momentum  $k_M$  used in micrometeorology to describe the momentum transfer in the atmosphere:

$$\varepsilon_a = k_M = \frac{\kappa u_* z}{\phi_m(z/L)} \quad (6)$$

Where  $\Phi_m(z/L)$  is the non-dimensional wind shear, which according to Monin-Obukhov theory only depends on the stability parameter  $z/L$ . The friction velocity  $u_*$  is related to the neutral ambient turbulence intensity  $I_{a,n}$  [4]:

$$u_* = \frac{\sigma_u}{2.4} = \frac{I_{a,n} u_0}{2.4} \quad (7)$$

For non-neutral conditions it is assumed that the ambient turbulence intensity  $I_a$  is related to the neutral one by  $I_a = I_{a,n} / \Phi_m(z/L)$ , i.e. the effect of stability on the ambient eddy-viscosity is already included in the ambient turbulence, which can be modelled as:

$$\varepsilon_a = \frac{\kappa u_* z}{\phi_m(z/L)} = \frac{\kappa \sigma_u z}{\phi_m(z/L) 2.4} = \frac{\kappa I_{a,n} u_0 z}{\phi_m(z/L) 2.4} = \frac{\kappa I_a u_0 z}{2.4} \quad (8)$$

The wake eddy-viscosity generated by the wind shear in the wake is modelled from the main length and velocity scales of the wake: its width  $r_w$  and centreline velocity deficit  $(u_0 - u_c)$ . For neutral atmospheric stability it is taken as:

$$\varepsilon_{w,n}(x) = kr_w(u_0 - u_c(x)) \quad (9)$$

Here  $k$  is a constant, which has to be found empirically. By comparisons using wind tunnel experiments with an axis-symmetric simulator with different thrust coefficients Ainslie estimated the value of  $k$  to be 0.015 [7].

In the experiments it was found that for small distances behind the rotor up to about 5 rotor diameters the wake eddy-viscosity was lower than expected from the above equation. This is attributed to the non-equilibrium of velocity and turbulence while the turbulence still develops and is modelled by introducing a filter function  $F(x)$ :

$$F(x) = 0.65 + \left( \frac{x - 4.5}{23.32} \right)^{1/3} \quad \text{for } x < 5.5 \quad (10)$$

For  $x > 5.5$   $F(x)$  is set to 1.

For an extension of the model to non-neutral stability it is assumed that the atmospheric stability acts in a similar way on both the turbulence in the surface layer and in the wake. Thus an approach similar to the ambient eddy-viscosity is taken:

$$\varepsilon_w(x) = \frac{\varepsilon_{w,n}(x)}{\Phi(z/L)} = \frac{kr_w(u_0 - u_c(x))}{\Phi(z/L)} \quad (11)$$

$\Phi_m(z/L)$  is calculated by the standard approach (see e.g. [4]) from the Monin-Obukhov length  $L$ , given as input, and the hub height  $z_H$ . Summarising the above equations, the total eddy-viscosity is modelled as<sup>1</sup>:

$$\varepsilon(x) = F\varepsilon_w(x) + \varepsilon_a = \frac{F(x)kr_w(u_0 - u_c(x))}{\Phi(z_H/L)} + \frac{\kappa u_0 z_H I_a}{2.4} \quad (12)$$

Note that the eddy-viscosity modelled in this way only depends on the distance to the rotor in  $x$  direction and is independent of the radial distance  $r$ .

The main simplification used in the model is the separation of wind shear and related eddy-viscosity of wake and ambient flow. This allows the two-dimensional description of the wake, which leads to a very efficient model. Not only the height dependence of the ambient eddy-viscosity is neglected, but more importantly the effect of calculating the eddy-viscosity separately for both parts, instead of calculating an eddy-viscosity from the local wind shear, which depends on both ambient and wake flow. For the atmospheric stability it is further assumed that its influence is equal for turbulence caused by vertical and horizontal wind speed gradients.

#### Boundary condition: Empirical wake profile at the end of the near wake

The near wake in the direct vicinity of the rotor can not be modelled with the simplified equations described above, since here the pressure gradients can not be neglected, but actually dominate the flow. Therefore the calculation of the wake is started at the end of the near wake, which in [7] is assumed to be at two rotor diameters distance behind the

---

<sup>1</sup> Note that there is a typing error in [7] (his equation 4), where the filter function is applied to both the wake and the ambient eddy-viscosity. The correct equation can be found in [18]

rotor. Here an empirical wake profile is used as boundary condition to solve the equations numerically. It was found from wind tunnel experiments and has been verified successfully with measurements on land. For the use in offshore conditions, further validation with measurements closer to the turbines is needed. However, the main characteristic of the offshore flow is a low turbulence intensity value, which is between the turbulence intensity levels of wind tunnel experiments and those encountered on land.

A Gaussian profile with centreline velocity deficit  $(u_0 - u_c)$  and wake width  $r_w$  is assumed, which is defined as the distance  $r_w$  at which the velocity deficit is 2.83% of its centreline value.

$$(u_0 - u_c) = c_t - 0.05 - (16c_t - 0.5) \frac{I}{10} \quad (13)$$

$$r_w = \sqrt{\frac{3.56c_t}{4(u_0 - u_c)(2 - (u_0 - u_c))}} \quad (14)$$

The velocity profiles  $u(r)$  and  $v(r)$  at the boundary  $x=x_n$  are then calculated using the continuity equation.

#### The near wake length

The length of the near wake  $x_n$  is modelled with an empirical approach following [13].

The near wake is divided in two regions, of which the first has the length  $x_H$ , which is modelled to be dependent on ambient turbulence, rotor generated turbulence and shear generated turbulence:

$$x_H = r_0 \left( \left( \frac{dr}{dx} \right)_\alpha^2 + \left( \frac{dr}{dx} \right)_\lambda^2 + \left( \frac{dr}{dx} \right)_m^2 \right)^{\frac{1}{2}} \quad (15)$$

where  $r_0$  is the effective radius of the fully expanded rotor disk:

$$r_0 = \frac{D}{2} \sqrt{\frac{m+1}{2}} \quad \text{with} \quad m = \frac{1}{\sqrt{1-c_t}} \quad (16)$$

$D$  is the rotor diameter and  $c_t$  is the thrust coefficient of the rotor. The influence of the different turbulence contributions is described as:

$$\left(\frac{dr}{dx}\right)_\alpha^2 = \begin{cases} 2.5I + 0.05 & \text{for } I \geq 0.02 \\ 5I & \text{for } I < 0.02 \end{cases} \quad \text{ambient turbulence} \quad (17)$$

$$\left(\frac{dr}{dx}\right)_\lambda^2 = 0.012B\lambda \quad \text{rotor generated turbulence} \quad (18)$$

$$\left(\frac{dr}{dx}\right)_m^2 = \frac{(1-m)\sqrt{1.49+m}}{9.76(1+m)} \quad \text{shear generated turbulence} \quad (19)$$

$I$  is the ambient turbulence intensity.  $B$  is the number of blades and  $\lambda$  the tip speed ratio.

Finally, the length of the near wake  $x_n$  is calculated from the length of the first region in the near wake by<sup>2</sup>:

$$x_n = \frac{\sqrt{0.212 + 0.145m}}{(1 - \sqrt{0.212 + 0.145m})} \frac{(1 - \sqrt{0.134 + 0.124m})}{\sqrt{0.134 + 0.124m}} x_H \quad (20)$$

This equation has a singularity at about  $c_t=0.97$ . For  $c_t>0.9$  the value of  $c_t$  is therefore set to 0.9 to avoid the singularity.

### Turbulence intensity

---

<sup>2</sup> after [19] – the equation given in [13] is erroneous

Not only the mean wind velocity is affected in a wind turbine wake, but also the fluctuations of the wind speed. Generally it has been found that the turbulence intensity is increased compared to the free stream flow. Apart from its importance for the development of the wake itself, the turbulence intensity is also the most important parameter for load calculations in wakes.

Two mechanisms are of main importance for the increase of turbulence intensity in the wake. From the flow pattern around the blades and at the tip the rotor produces a rotor-generated turbulence. It is most important in the near wake directly behind the rotor. Since the near wake is not modelled here this turbulence contribution is only indirectly included in the calculation via the empirical near wake length and incident wake profile. The second contribution is the shear-generated turbulence, stemming from the wind shear in the wind speed profile of the wake.

The wind shear in the wake produces additional wake turbulence in a similar way as the wind shear in the atmospheric surface layer produces the ambient turbulence. Since wind shear and eddy-viscosity are closely related, we assume that the ratio between eddy-viscosity and turbulence intensity (see equation 8) can also be used for the wake turbulence intensity, only in the opposite way. Instead of calculating the ambient eddy-viscosity from the ambient turbulence intensity now the wake turbulence intensity is calculated from the wake eddy-viscosity:

$$I = \varepsilon \frac{2.4}{\kappa u_0 z_H} \quad (21)$$

Note that the wake turbulence intensity is here defined as  $\sigma_w/u_0$ , i.e. with reference to the free wind speed. The influence of atmospheric stability on the turbulence intensity in the wake is automatically included by using this eddy-viscosity.

## 2.4 Wind farm model

The single wake model estimates the flow velocity in the wake. To estimate the average wind speed over the rotor the momentum deficit is averaged over the rotor area:

$$(u_0 - u_{Rotor})^2 = \frac{1}{A_{Rotor}} \int (u_0 - u_w)^2 dA \quad (22)$$

The influence of multiple wakes on the wind speed of the rotor area is calculated by adding the momentum deficits of all incident wakes and integrating over the rotor area:

$$(u_0 - u_{Rotor})^2 = \frac{1}{A_{Rotor}} \int \sum_{i, \text{all wakes}} (u_{Rotor(i)} - u_{w(i)})^2 dA \quad (23)$$

Here the momentum deficit of one incident wake is defined as the square of the difference of the averaged wind speed before the rotor producing the wake and the wind speed in the wake.

From the mean wind speed of the rotor area  $u_{Rotor}$ , with all wakes taken into account, the power output of a turbine is estimated from its power curve.

## 3 The Vindeby Measurements

### 3.1 Vindeby wind farm

Vindeby wind farm was built in 1991 in the Baltic Sea off the coast of Denmark, about 2 km off the north-west coast of the island of Lolland (see Figure 1). The distance of the turbines to the land is between 1.5 km and 2.7 km. The water depth is between 2 and 5 m. The wind farm consists of 11 Bonus 450 kW wind turbines, arranged in two rows oriented along an axis of 325-145° (see Figure 1). The distance of the turbines within

the row as well as the distance between the rows is 300 m (8.6 D). Since the turbine locations are shifted in the two rows with respect to each other, the minimum distance between turbines of two rows is 335 m (9.6 D).

The turbines are stall regulated Bonus 450 kW turbines with hub height 38 m and rotor diameter 35 m. Their thrust coefficient curve is shown in Figure 2 as supplied by the manufacturer. For a detailed description of the wind farm and measurements see [14] and [15].

### 3.2 Measurements and instrumentation

Three meteorological masts have been erected close to the wind farm, one on land and two offshore. The land mast is located at the coast nearly 2 km south of the most southerly turbine in the array. The two offshore masts are placed at distances equal to the row and turbine spacing (335 and 300 m), one to the west and one to the south of the first row. The locations of the masts with respect to the wind turbines are shown in Figure 1. The minimum distances from land to sea mast south (SMS) and sea mast west (SMW) are approximately 1.3 km and 1.6 km, respectively.

Wind speed measurements with cup anemometers are performed at 46, 38, 20 and 7 m height at the land mast (LM) and at 48, 43, 38, 29, 20, 15 and 7 m height at SMS and SMW. The atmospheric stability is characterised by the Monin-Obukhov length  $L$ , which is derived from temperature and wind speed difference measurements at the three masts.

### 3.3 Data compilation

Measurement data from Vindeby wind farm from the years 1994 and 1995 have been used. One minute averages have been calculated for all data, resulting in a data base of 466116 observations [10].

For comparison of the model with measurements, four wind direction cases of direct wake interference were selected where measurements of the wind speed in the wake as well as measurements of the free wind speed are available (see Table 1). For the selection of the data the wind direction at the wake mast was used. For each of the cases data have been classified according to criteria: wind speed, turbulence intensity and atmospheric stability at the free mast. Wind speed bins of  $4-6\text{ms}^{-1}$ ,  $6-9\text{ms}^{-1}$ ,  $9-11\text{ms}^{-1}$  and above  $11\text{ms}^{-1}$ , turbulence intensity bins of 5-7%, 7-9%, 9-11% and above 11%, and atmospheric stability bins of  $|L|>1000$ ,  $0<L<1000$ ,  $0>L>-1000$  have been used. The stability was determined at the free mast (LM at  $23^\circ$  and SMS at  $77^\circ$ ), except for the  $320^\circ$  case, where the stability of the LM is used. For each case and each bin the data were averaged and normalised with the corresponding free stream wind velocity at hub height (38 m) (see [10]).

### 3.4 Measurement uncertainties

The comparison of measured and modelled wakes is very sensitive to measurement uncertainties in the wind speed measurements since the modelled wake deficit has to be compared with a measurement of a wind speed *difference* (wind speed in the free stream and in the wake).

Four main sources of systematic errors have been identified:

- calibration uncertainty leading to offsets between the anemometers
- uncertainty of the measurement accuracy of the anemometer in turbulent flow
- flow distortion around the mast and boom, leading to a wind speed enhancement for wind directions close to the sector of direct mast shade and a wind speed decrease for wind directions opposite to the mast shade direction
- direct mast shade, leading to a wind speed decrease

These systematic measurement uncertainties have been investigated by comparison of wind speed measurements of different anemometers at the same height for wind directions with undisturbed flow. Wind speed differences of up to 4% were found.

It has also been investigated if the anemometers are influenced by direct mast shade. The single wake case in wind direction  $23^\circ$  is taken as an example. The free wind speed is in this case measured with the LM, which has a boom direction of  $350^\circ$ . Wind directions from  $18^\circ$  to  $28^\circ$  measured at SMS are used to determine the wake deficit. At 38 m height two anemometers are mounted on opposite sides of the mast.

In Figure 3 the wind speed ratio between the south and north anemometer at LM is shown versus the wind direction at SMS. The beginning of the direct mast shade can clearly be seen for wind direction angles smaller than  $15^\circ$ . It can be seen that the mast shade has no influence on the measurement for the wind direction sector of the wake measurement ( $18^\circ$  to  $28^\circ$ ). However, the ratio of the wind speeds in the wake sector is about 1.03, i.e. the south anemometer measured a wind speed, which is about 3% higher than the north anemometer. This is believed to be mainly caused by flow distortion around the mast and boom, as described in [16]. Comparisons of wind speeds measured at both sides of the three masts showed that the influence of the direct mast shade on the

anemometers for the wind directions used in the wake cases (see Table 1) is small. It is estimated to be below 2%.

In the data analysis an additional uncertainty is introduced when the distribution of measured values within a wind speed, turbulence intensity or stability bin is biased. This leads to a deviation of the bin average to its nominal value.

The total uncertainty in the measured wind speeds for comparison with the modelled wakes is estimated to be in the order of +/-5%.

## 4 Results of the Comparison

### 4.1 Free flow profiles

The measured wind speeds of the free mast, bin-averaged and normalised as described in section 3.3, are compared with the model of the free vertical wind speed profile (see section 2.2). Data for the three different cases of wind direction sectors (18°-28°, 70°-78° and 314°-323°) are used.

A subset of the results is shown in Figure 4. Measured and modelled free flow profiles are shown for the bin with turbulence intensity 6% and wind speed  $7.5 \text{ ms}^{-1}$ . Results for the three stability classes are compared. For near-neutral and unstable atmospheric conditions the measured and modelled free flow profiles agree well. For stable conditions large deviations are found between the different measurements (wind direction sectors) and also between one of the measurements and the model.

A possible explanation for the problems in stable stratification are flow modifications, which might occur when warmer air is advected for a long distance over colder sea.

Under certain conditions an inversion layer develops, leading to a vertical wind speed profile that does not follow Monin-Obukhov theory (see e.g. [20]). A similar behaviour has recently been found at the Rødsand measurement, which is located less than 100 km from Vindeby, south of the island Lolland [21].

## 4.2 Wake profiles

### Method of comparison

Vertical profiles of bin-averaged measurement data are used for comparisons with model calculations. Single wakes, double wakes, i.e. wakes of a turbine that itself is in a wake of a second upwind turbine, and quintuple wakes (5 turbines in a row) are used in the comparison (see section 3.3 and Table 1).

The measurement data are bin-averaged. For turbulence intensity, wind speed and stability the nominal (mid-bin) values are used as input to the model. For wind direction the averaging has been repeated in the modelling by running the model for the range of directions used in the averaging in  $1^\circ$  steps and averaging the model results.

The reason is illustrated in Figure 5, which shows a modelled horizontal profile of a single wake hub height (38 m) under a 6% turbulence regime, neutral atmospheric stability and a wind speed of  $5 \text{ ms}^{-1}$ . The normalised wind speed is plotted versus wind direction. The vertical lines indicate the averaged wind direction range and the horizontal line is the average of the modelled velocity deficit for the range used in the measurements. In this example the averaged normalised wake deficit is 0.13, while the maximum wake deficit is 0.17, which is a difference of about 30%.

For multiple wakes the modelling has been simplified by neglecting the effect of the increase in turbulence intensity in a wake. Instead, the ambient turbulence intensity has been used for all wakes.

#### Comparison for near neutral stability

Examples of the comparison for single, double and quintuple wake situations in near-neutral atmospheric conditions are given in Figure 6, Figure 7 and Figure 8, respectively, for the most frequent turbulence intensity bin, 6%, and the most frequent wind speed bins,  $5 \text{ ms}^{-1}$  and  $7.5 \text{ ms}^{-1}$ .

Model results are within the estimated measurement uncertainty for all scenarios. It can be noted, however, that larger deviations occur for the double wake situations (Figure 7), which are measured in two different wind direction cases. Large differences can be seen between these two measured profiles. The measurements for the  $70^\circ$ - $78^\circ$  case show large velocity deficits at low heights, even down to 7 m, while the measurements for the  $18^\circ$ - $28^\circ$  case show generally smaller wake deficits.

#### Comparison for stable conditions

Figure 9 shows examples for stable atmospheric stratification for single, double and quintuple wake situations for 6% turbulence intensity and 5 m/s for single and 7.5 m/s for multiple wakes. As for the comparison of the free flow models (see section 4.1), the comparison of model results with measurements for stable stratification shows larger deviations than for near-neutral stratification.

For the single and quintuple wake cases it can be seen that the wind shear of the free flow is already underestimated. As the free flow is a part of the modelled wake this is also present in the wake model result.

In the single wake case the measured wind speed shows an unexpected profile with a maximum at 30 m height which can not be explained. For the double wake case the measured wind shear is larger than modelled. This has already be found in the near-neutral cases for this direction. For the quintuple wake case the deviation of the free flow model from the measured free flow is similar to the deviation of modelled and measured wake.

#### Comparison for unstable conditions

Figure 10 shows examples for the comparison of single, double and quintuple wake situations with measurements for 6% turbulence intensity and  $7.5 \text{ ms}^{-1}$  mean wind speed in unstable atmospheric conditions. As for stable conditions, the comparison of model results with measurements for unstable stratification is not as good as for near-neutral stratification. While a good agreement is found for the single wake case, double and quintuple wakes show large deviations. For the double wake case the model overpredicts the wake deficit, while for the quintuple wake case a slight underprediction of the wake deficit can be seen. Additionally, for the quintuple wake the measured free flow profile has a larger wind shear than modelled, which was also found for stable stratification.

For the double wake in the  $70^\circ$ - $78^\circ$  wind direction the wind shear deviates between model and measurement. This was also found in all other comparisons for this wind direction case. The reason for this deviation is unknown, but a height dependent systematic error due to mast shade is a possible explanation. Since the mast cross section increases from top to bottom, the wind direction range influenced by the mast shade can be expected to increase. This could cause a height dependent wind speed error, which increases from top to bottom.

### 4.3 Turbulence intensity

The turbulence intensity is calculated as the standard deviation of the wind speed measured in the wake divided by the mean ambient wind speed measured at the free mast. This is the definition of the turbulence intensity used in the model (see equation 20). It should be noted that the turbulence intensities are measured for a 1-minute averaging period rather than the usual 10 minutes. However, this has only an influence on the absolute values and not on the comparison, since the ambient turbulence intensity is measured in the same way here.

The measured and modelled turbulence intensities in a single wake for the 18°-28° case of Vindeby wind farm at 38 m height are compared in Table 2 and Figure 11. For comparison the wake turbulence intensities have also been modelled with the commonly used empirical formula by Quarton and Ainslie [17] (see Table 2).

The measured turbulence intensities show only a small dependency on ambient conditions like wind speed, atmospheric stability or ambient turbulence intensity. The average standard deviation of the measurements within the bins is 3%, which is larger than the differences for different ambient conditions. The measured turbulence intensity can therefore be characterised by its mean value, which is 8.5%. The predicted mean turbulence intensity of the wake model is 8.9% and that of the empirical formula is 7.8%.

Both approaches predict an influence of ambient conditions on the wake turbulence intensity, especially of ambient turbulence intensity, but also of atmospheric stability and (less important) wind speed. These dependencies are the same for both models. The main difference is that the wake model generally predicts a slightly higher turbulence

intensity in the wake. On average, this compares better with the measurements than the results of the empirical formula.

## 5 Conclusion

The wind farm layout program FLaP has been extended to improve the capability to model offshore wind farms. The characteristics of the offshore atmospheric flow most important for wind power utilisation have been addressed: Sea surface roughness and atmospheric stability.

Model performance has been compared with measurement results from the Vindeby offshore wind farm. The measurement uncertainty for the bin-averaged wind speed measurements in narrow wind direction sectors has been estimated to about 5%. Since wake deficit measurements are measurements of wind speed *differences* this leads to large uncertainties in the comparison.

The improved FLaP model agrees well with the measurements for the atmospheric conditions, which are most important for wind power utilisation. These are the conditions with important energy content and high frequency of occurrence, i.e. moderate wind speeds, typical turbulence intensities and near-neutral stability.

The model coped well with the low turbulence intensity offshore as no significant deviations were found for low turbulence situations. Modelling was less successful when atmospheric stability deviated from near-neutral conditions. This was the case both for stable and unstable stratification and both for the modelling of the free profile and the wake flow. This shows that the behaviour of free and wake flows in conditions

with non-neutral atmospheric stratification is not understood sufficiently and needs further investigation.

The measurements of turbulence intensity in wakes showed only a small dependency on ambient conditions, especially on the ambient atmospheric stability. Since a dependency on ambient conditions is usually assumed and also modelled, some deviations occur. However, the variation within the measurement is larger than the differences in question and more detailed measurements are needed here.

## Acknowledgement

Financial support for this research was given in part by the European Commission's Fifth Framework Programme under the Energy, Environment and Sustainable Development Programme. Project Reference: ERK6-1999-00001 ENDOW (Efficient Development of Offshore Windfarms).

## References

1. PARK. Computer Program. Risø National Laboratory, Roskilde, Denmark
2. Windfarmer. Computer Program. Garrad and Hassan, Bristol, United Kingdom
3. FLaP. *Farm Layout Program, University of Oldenburg, Germany* 1996. (see [www.physik.uni-oldenburg.de/ehf/](http://www.physik.uni-oldenburg.de/ehf/))
4. Lange B, Højstrup J, Larsen SE, Barthelmie RJ. A fetch dependent model of sea surface roughness for offshore wind power utilisation. *Proceeding of the European Wind Energy Conference 2001, Copenhagen, Denmark* 2001; 830-833.

5. Stull RB. *An Introduction to Boundary Layer Meteorology*. Dordrecht, Boston, London, Kluwer Academic Publishers. 1988.
6. Charnock H. Wind stress over a water surface. *Quart. J. Roy. Meteor. Soc* 1955; **81**: 639-640.
7. Ainslie JF. Calculating the flowfield in the wake of wind turbines. *Journal of Wind Engineering and Industrial Aerodynamics* 1988; **27**: 213-224.
8. Rados K, Schlez W, Lange B, Schepers G, Hegberg T, Magnusson M. Comparison of wake models with data. *Wind Engineering* 2002: (accepted for publication). (as workshop proceeding available at [www.risoe.dk/vea/projects/endow](http://www.risoe.dk/vea/projects/endow))
9. Schlez WA, Umaña EA, Barthelmie RJ, Larsen G, Jørgensen H, Rados K, Bergström H, Magnusson M, Lange B, Vølund P, Neckelmann S, Schepers G, Hegberg T. ENDOW: Improvement of wake models. *Wind Engineering* 2002: (accepted for publication). (as workshop proceeding available at [www.risoe.dk/vea/projects/endow](http://www.risoe.dk/vea/projects/endow))
10. Barthelmie RJ, Larsen G, Jørgensen H, Rados K, Bergström H, Magnusson M, Hassan U, Schlez W, Lange B, Vølund P, Neckelmann S, Christensen L, Højstrup J, Schepers G, Hegberg T, Folkerts L, Coelingh J. ENDOW: Efficient development of offshore windfarms. *Wind Engineering* 2002: (accepted for publication). (as workshop proceeding available at [www.risoe.dk/vea/projects/endow](http://www.risoe.dk/vea/projects/endow))
11. Waldl HP. *Modellierung der Leistungsabgabe von Windparks und Optimierung der Aufstellungsgeometrie*. PhD thesis at the University of Oldenburg; 175p. 1988. (in German)

12. Wu J. Wind-stress Coefficients over Sea Surface near Neutral Conditions – A Revisit. *J. Phys. Oceanogr.* 1980; **10**: 727-740.
13. Vermeulen PEJ. An experimental analysis of wind turbine wakes. *Proceedings of the International Symposium on Wind Energy Systems, Lyngby, Denmark*; 1980; 431-450.
14. Frandsen S, Chacón L, Crespo A, Enevoldsen AP, Gómez-Elvira R, Hernández J, Højstrup J, Manuel F, Thomsen K, Sorensen P. Measurements on and Modelling of Offshore Wind Farms, *Report Risø-R-903(EN), Risø National Laboratory, Denmark* 1996
15. Barthelmie RJ, Courtney MS, Højstrup J, Larsen SE. Meteorological aspects of offshore wind energy: Observations from the Vindeby wind farm. *Journal of Wind Engineering and Industrial Aerodynamics* 1996; **62**: 191-211.
16. Højstrup J. Vertical Extrapolation of Offshore Windprofiles. *Wind energy for the next millennium. Proceedings. 1999 European wind energy conference (EWEC '99), Nice (FR). Petersen, E.L.; Hjuler Jensen, P.; Rave, K.; Helm, P.; Ehmann, H., Eds.,* 1999; 1220-1223
17. Quarton DC, Ainslie JF. Turbulence in wind turbine wakes. *Wind Engineering* 1990; **14 (1)**: 15-23.
18. Ainslie JF. Development of an Eddy Viscosity Model for Wind Turbine Wakes. *7th BWEA Wind Energy Conference, Oxford, U.K.* 1985.
19. Schlez W. Vermessung und Analyse der Abströmung einer Windenergieanlage im Windpark Norddeich. *MSc. thesis at the University of Oldenburg* 1992. (in German)

20. Csanady GT, Equilibrium theory of the planetary boundary layer with an inversion lid. *Boundary-Layer Meteorol.* 1974; **6**: 63-79.
21. Lange B, Larsen S, Højstrup J, Barthelmie R. The influence of thermal effects on the wind speed profile of the coastal marine boundary layer. submitted to *Boundary-Layer Meteorol.* 2002

## Figure captions

Figure 1: Location of Vindeby wind farm in the Baltic Sea in the southern part of Denmark and layout of the Vindeby wind farm and the measurement masts

Figure 2: Thrust coefficient curve for the Bonus 450 kW turbine

Figure 3: Ratio between the wind speeds (WS) measured by the north and south anemometer at 38 m height the LM versus wind direction (WD) measured at the SMS

Figure 4: Measured and modelled free vertical wind speed profile for near neutral stratification ( $L > 1000$ ) (left), stable stratification ( $0 < L < 1000$ ) (middle) and unstable stratification ( $0 > L > -1000$ ); turbulence intensity bin 6% (5-7%), wind speed bin  $7.5 \text{ ms}^{-1}$  ( $6-9 \text{ ms}^{-1}$ ), wind direction sectors as used for wake comparisons; error bars indicate the standard errors

Figure 5: Wind direction dependent (horizontal) wake modelling at hub height for the case of 6% turbulence intensity, neutral atmospheric stability and a wind speed of  $5 \text{ ms}^{-1}$ ; the dashed line shows the average for the wind direction sector  $18^\circ$  to  $28^\circ$

Figure 6: Vertical profiles of measured and modelled normalised wind speeds for the free and wake flow; Vindeby single wake with wind direction  $18^\circ$ - $28^\circ$ , near-neutral stability, 6% turbulence intensity,  $7.5 \text{ ms}^{-1}$  (170 records) and  $10 \text{ ms}^{-1}$  (59) mean wind speed; error bars indicate the standard errors

Figure 7: Vertical profiles of measured and modelled normalised wind speeds for the free and wake flow; Vindeby double wake with wind direction  $70^\circ$ - $78^\circ$  and  $18^\circ$ - $28^\circ$ , near-neutral stability, 6% turbulence intensity,  $7.5 \text{ ms}^{-1}$  (18-28: 170 records; 70-77: 254) and  $10 \text{ ms}^{-1}$  (18-28: 59; 70-77: 332) mean wind speed; error bars indicate the standard errors

Figure 8: Vertical profiles of measured and modelled normalised wind speeds for the free and wake flow; Vindeby quintuple wake with wind direction  $314^{\circ}$ - $323^{\circ}$ , near-neutral stability, 6% turbulence intensity,  $7.5\text{ms}^{-1}$  (420 records) and  $10\text{ms}^{-1}$  (344) mean wind speed; error bars indicate the standard errors

Figure 9: Vertical profiles of measured and modelled normalised wind speeds for the free and wake flow; Vindeby single (67 records), double (101) and quintuple (43) wakes, stable stratification, 6% turbulence intensity,  $5\text{ms}^{-1}$  (single) and  $7.5\text{ms}^{-1}$  (double and quintuple) mean wind speed; error bars indicate the standard errors

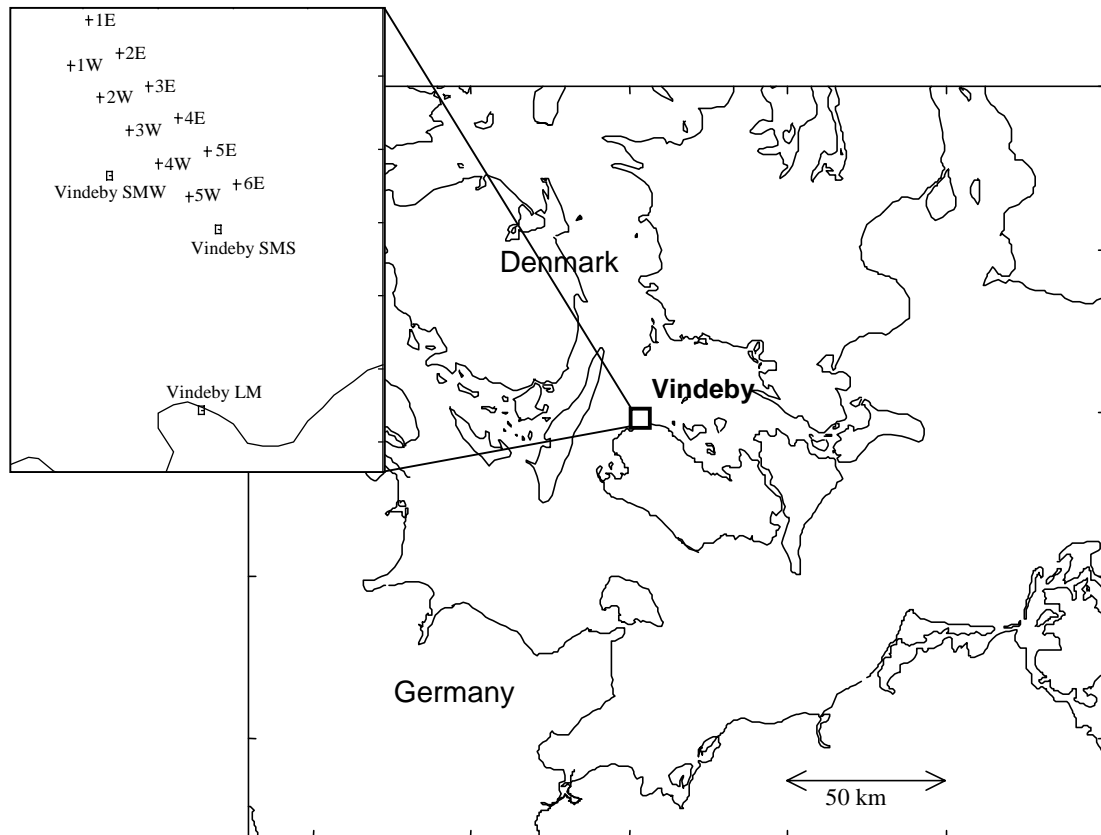
Figure 10: Vertical profiles of measured and modelled normalised wind speeds for the free and wake flow; Vindeby single (86 records), double (65) and quintuple (275) wakes, unstable stratification, 6% turbulence intensity,  $7.5\text{ms}^{-1}$  mean wind speed; error bars indicate the standard errors

Figure 11: Measured versus modelled turbulence intensity in the single wake

## Table captions

Table 1: Measured wake cases at Vindeby wind farm

Table 2: Measured and modelled (m=measured, w=wake model, e=empirical formula)  
turbulence intensities in % in the single wake at Vindeby wind farm; 18°-28° case,  
9.6D distance, 38m height



*Figure 1: Location of Vindeby wind farm in the Baltic Sea in the southern part of Denmark and layout of the Vindeby wind farm and the measurement masts*

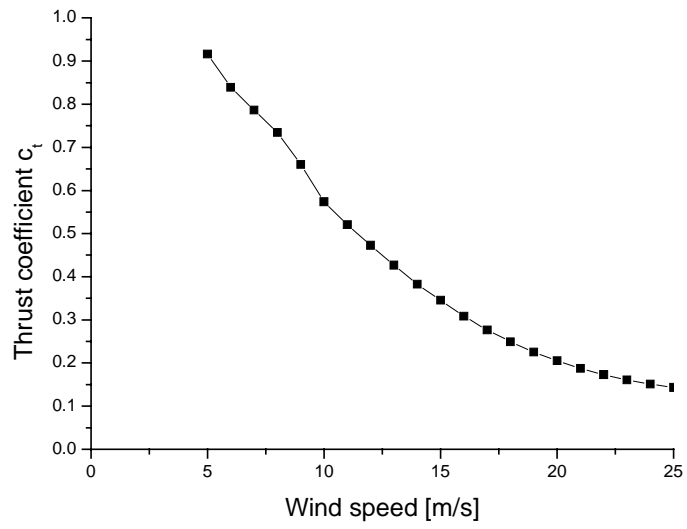


Figure 2: Thrust coefficient curve for the Bonus 450 kW turbine

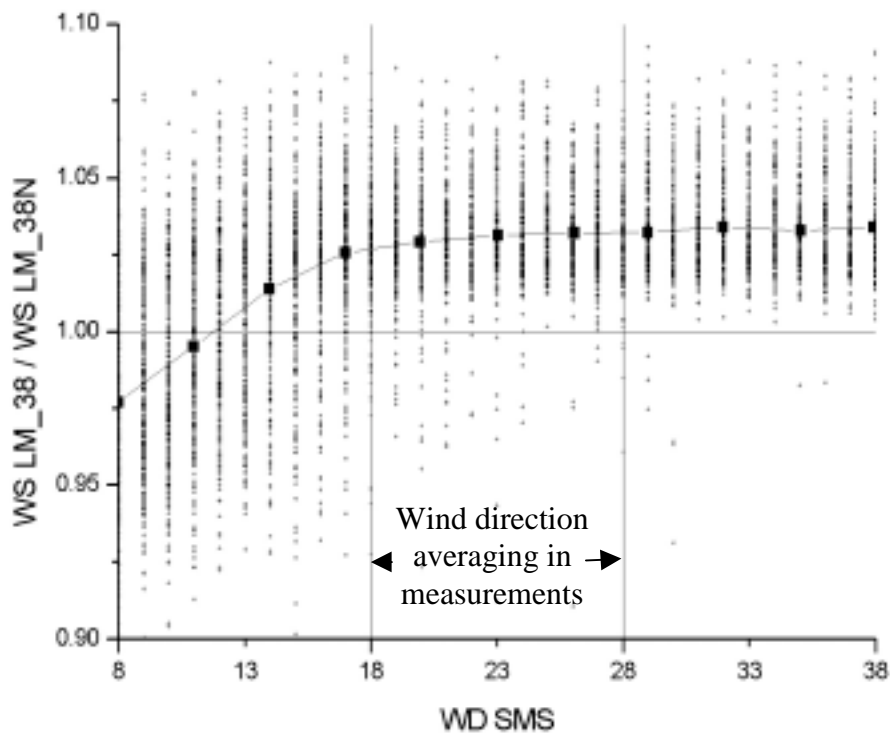


Figure 3: Ratio between the wind speeds (WS) measured by the north and south anemometer at 38 m height the LM versus wind direction (WD) measured at the SMS

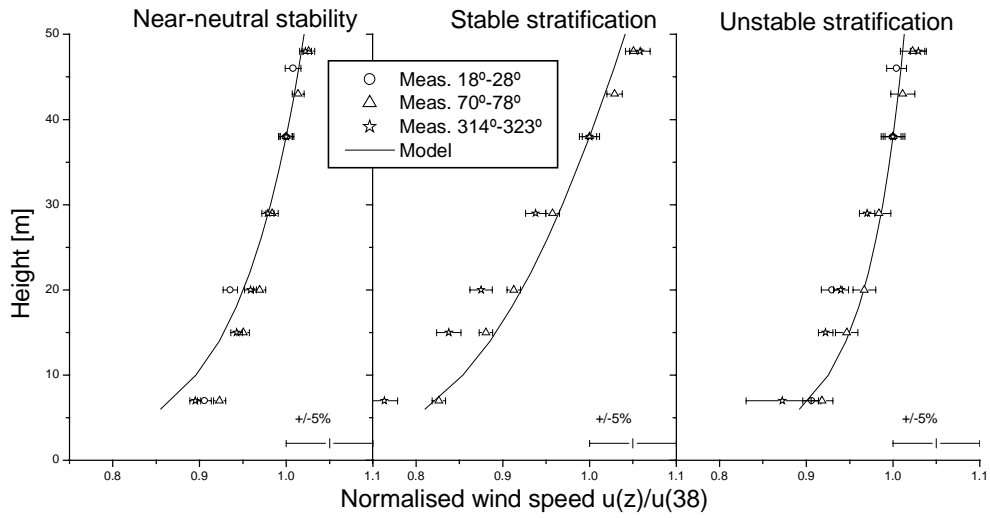


Figure 4: Measured and modelled free vertical wind speed profile for near neutral stratification ( $|L| > 1000$ ) (left), stable stratification ( $0 < L < 1000$ ) (middle) and unstable stratification ( $0 > L > -1000$ ); turbulence intensity bin 6% (5-7%), wind speed bin  $7.5 \text{ms}^{-1}$  ( $6-9 \text{ms}^{-1}$ ), wind direction sectors as used for wake comparisons; error bars indicate the standard errors

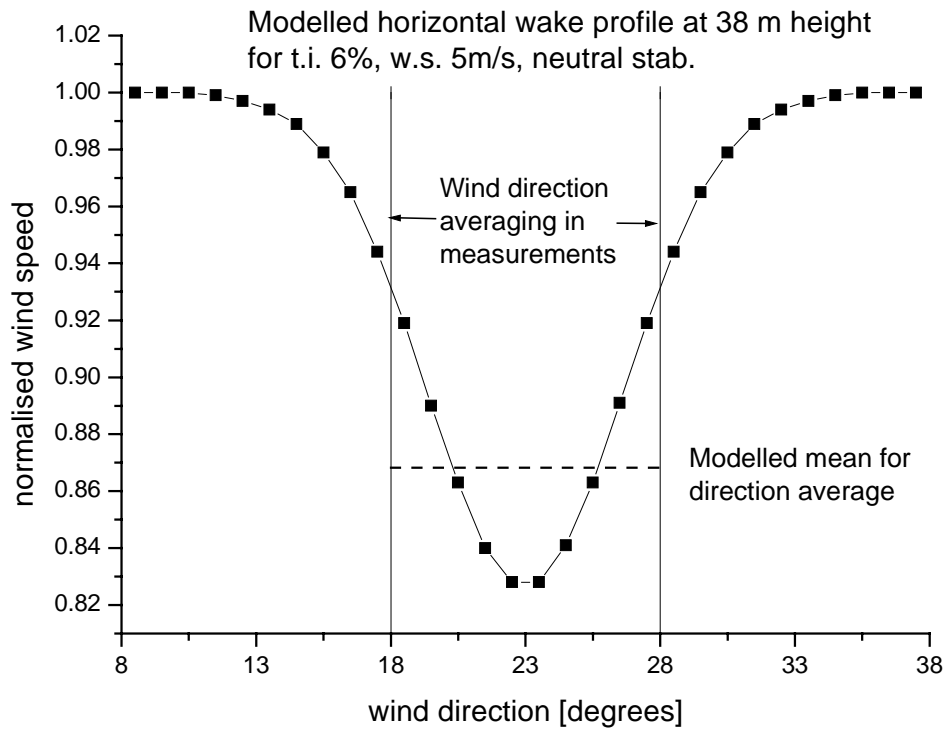


Figure 5: Wind direction dependent (horizontal) wake modelling at hub height for the case of 6% turbulence intensity, neutral atmospheric stability and a wind speed of  $5 \text{ ms}^{-1}$ ; the dashed line shows the average for the wind direction sector  $18^\circ$  to  $28^\circ$

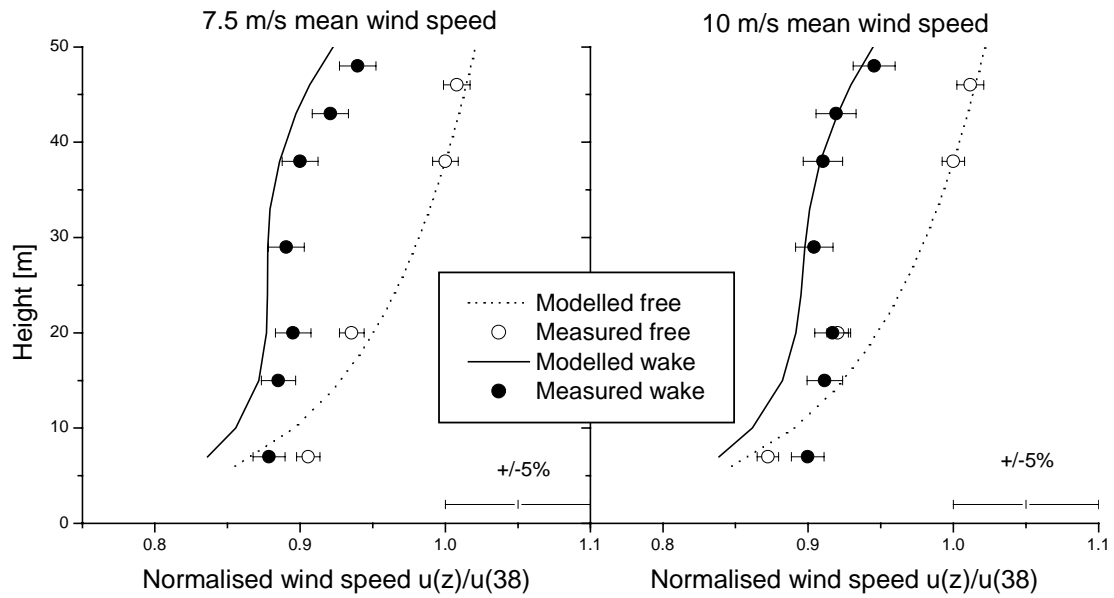


Figure 6: Vertical profiles of measured and modelled normalised wind speeds for the free and wake flow; Vindeby single wake with wind direction  $18^{\circ}$ - $28^{\circ}$ , near-neutral stability, 6% turbulence intensity,  $7.5\text{ms}^{-1}$  (170 records) and  $10\text{ms}^{-1}$  (59) mean wind speed; error bars indicate the standard errors

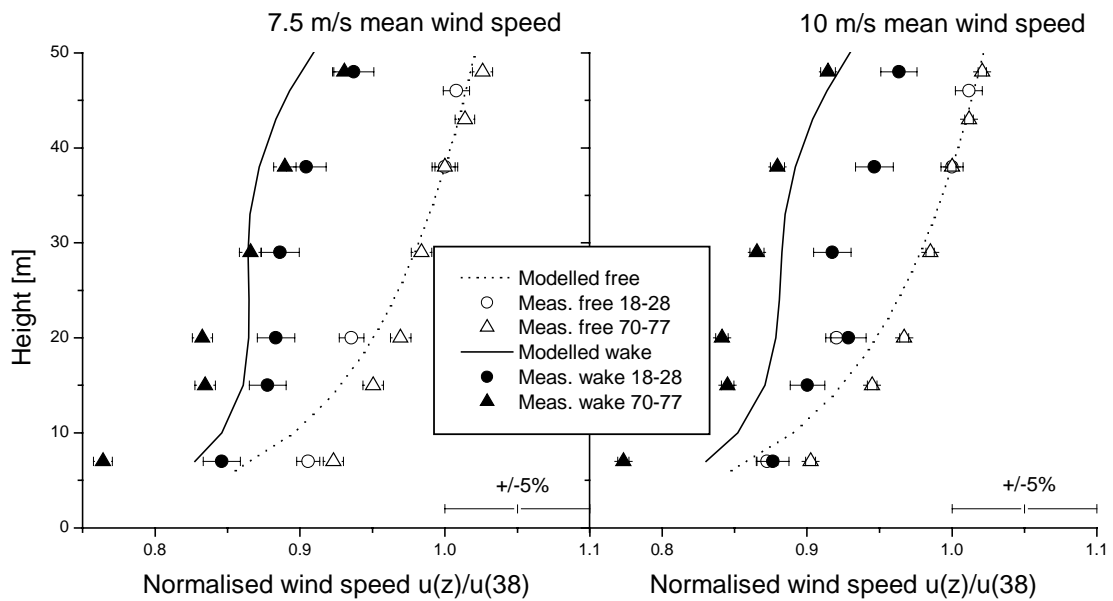


Figure 7: Vertical profiles of measured and modelled normalised wind speeds for the free and wake flow; Vindeby double wake with wind direction  $70^{\circ}$ - $78^{\circ}$  and  $18^{\circ}$ - $28^{\circ}$ , near-neutral stability, 6% turbulence intensity,  $7.5\text{ms}^{-1}$  (18-28: 170 records; 70-77: 254) and  $10\text{ms}^{-1}$  (18-28: 59; 70-77: 332) mean wind speed; error bars indicate the standard errors

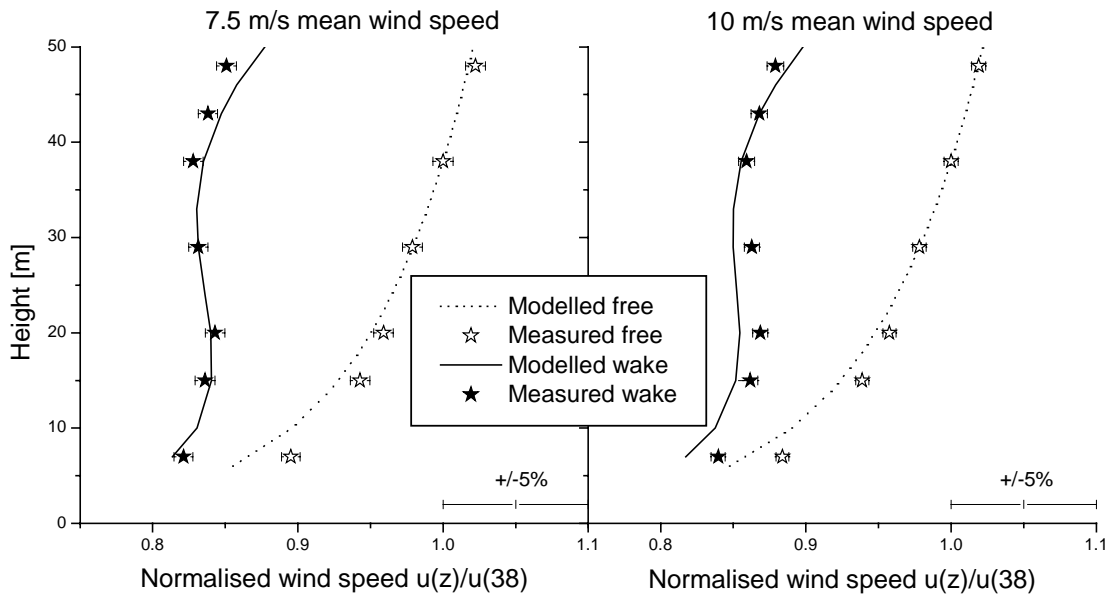


Figure 8: Vertical profiles of measured and modelled normalised wind speeds for the free and wake flow; Vindeby quintuple wake with wind direction  $314^{\circ}$ - $323^{\circ}$ , near-neutral stability, 6% turbulence intensity,  $7.5\text{ms}^{-1}$  (420 records) and  $10\text{ms}^{-1}$  (344) mean wind speed; error bars indicate the standard errors

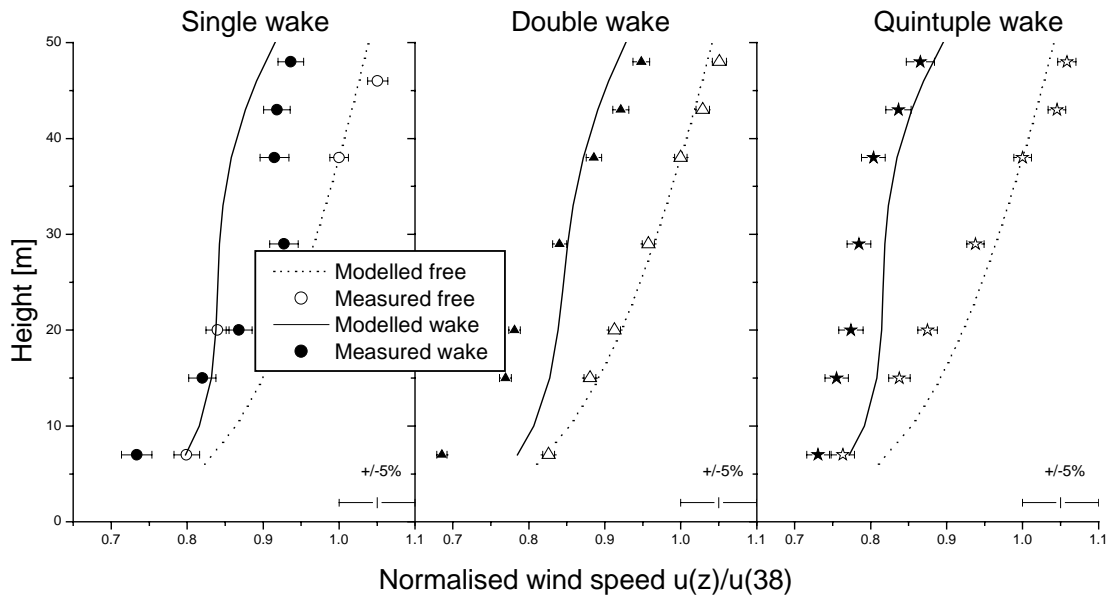


Figure 9: Vertical profiles of measured and modelled normalised wind speeds for the free and wake flow; Vindeby single(67 records), double (101) and quintuple (43) wakes, stable stratification, 6% turbulence intensity,  $5\text{ms}^{-1}$  (single) and  $7.5\text{ms}^{-1}$  (double and quintuple) mean wind speed; error bars indicate the standard errors

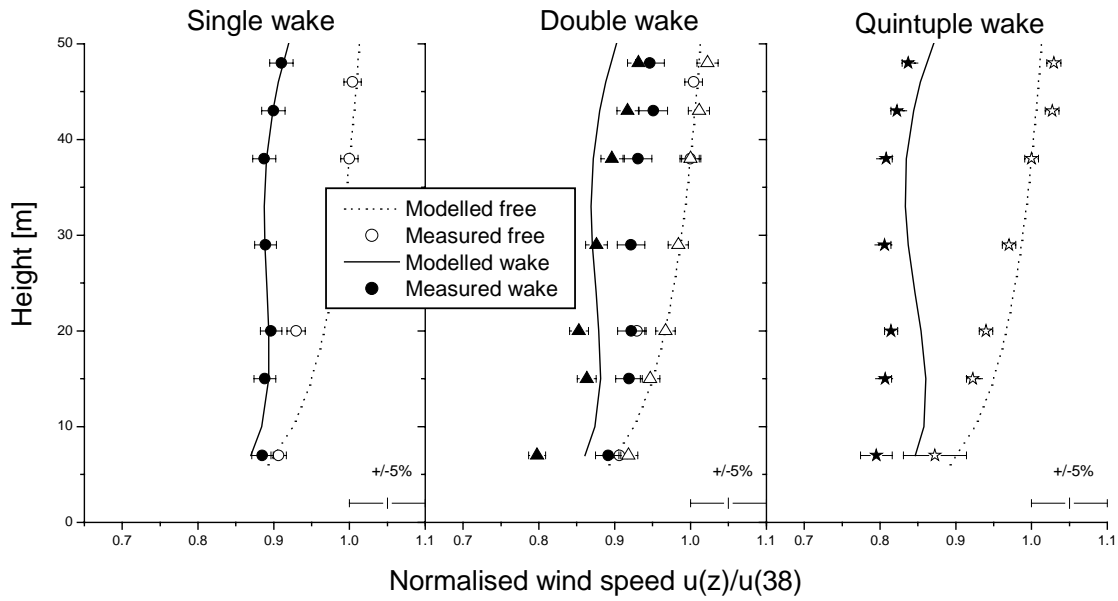


Figure 10: Vertical profiles of measured and modelled normalised wind speeds for the free and wake flow; Vindeby single (86 records), double (65) and quintuple (275) wakes, unstable stratification, 6% turbulence intensity,  $7.5\text{ms}^{-1}$  mean wind speed; error bars indicate the standard errors

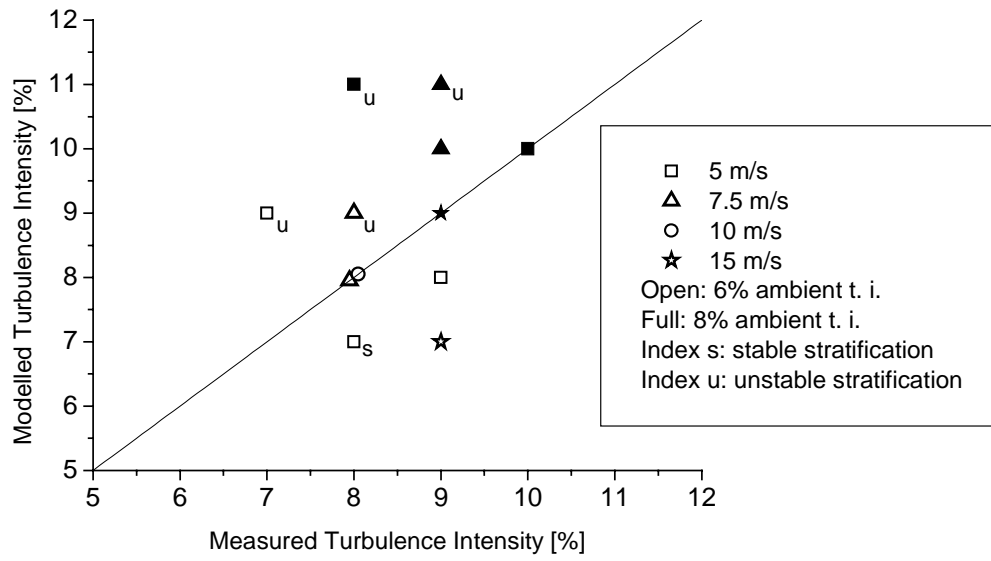


Figure 11: Measured versus modelled turbulence intensity in the single wake

*Table 1: Measured wake cases at Vindeby wind farm*

case	wind direction sector	wake type	free mast	wake mast	stability determined from
s-23	18°-28°	single	LM	SMS	LM
d-23	18°-28°	double	LM	SMW	LM
d-77	70°-78°	double	SMS	SMW	SMS
q-314	314°-323°	quintuple	SMW	SMS	LM

*Table 2: Measured and modelled (m=measured, w=wake model, e=empirical formula) turbulence intensities in % in the single wake at Vindeby wind farm; 18°-28° case, 9.6D distance, 38m height*

		5ms <sup>-1</sup>			7.5ms <sup>-1</sup>			10ms <sup>-1</sup>			15ms <sup>-1</sup>		
		m	w	e	m	w	e	m	w	e	m	w	e
6%	neutral	9	8	7	8	8	7	8	8	7	9	7	6
	stable	8	7	7									
	unstable	7	9	8	8	9	7						
8%	neutral	10	10	9	9	10	9				9	9	8
	stable												
	unstable	8	11	10	9	11	9						